sustainability

Article

The Relationships between Urbanization, Altitude Variability and Disaster Risk Management, Evidence from Jordan

Rania Qutieshat [1,*] and Tasneem Al-Assaf [2]

1 Planning and Project Management Department, Faculty of Business, Al-Balqa Applied University, As-Salt 19117, Jordan
2 Jordan Ministry of Local Administration, Al Mafraq 25823, Jordan; tasneem.alassaf@outlook.com
* Correspondence: qutieshat@bau.edu.jo

Abstract: This study was conducted in Jordan to assess the relationships between built environment (population growth, green surfaces, and built-up land), altitude variability, and landslide events during the period 1994 to 2020 through the application of a multi-approach investigation using statistical analyses, GIS, and remote sensing techniques. The results showed that the population densities in the study area have substantially increased. The population in the northern parts is distributed along an east–west direction that moves anticlockwise toward the south, while the southern parts population distribution is along a north–south direction that moves clockwise and to the south. The normalized difference vegetation index (NDVI) results showed that the green surfaces in the study area have decreased by 4.6%, while the built-up land density has increased. The landslide events increased from four events in 1994 to more than 20 events in 2020. There is a synchronous pattern in which the decrease in vegetation is associated with an increase in built-up land, population size, and landslide events at different altitudes, suggesting that a relationship between these factors might be present. If the current built environment practices persist, the population distribution and concentration will spread in a north-south direction along the same axis where landslide events are concentrated, posing serious future potential hazards on the population and on facilities.

Keywords: Jordan; landslide; population growth; regional planning; urban sprawl

check for updates

Citation: Qutieshat, R.; Al-Assaf, T. The Relationships between Urbanization, Altitude Variability and Disaster Risk Management, Evidence from Jordan. *Sustainability* **2022**, *14*, 9241. https://doi.org/10.3390/su14159241

Academic Editor: Giuseppe T. Cirella

Received: 5 June 2022
Accepted: 17 July 2022
Published: 28 July 2022

1. Introduction

Planning indicates, primarily, a systematic approach that addresses and explores a problem through specific objectives and methodologies [1]. Regional planning, which aims to maximize the most suitable and sustainable usage of a given physical area [2], encompasses several aspects, including land use/land cover (LU/LC) planning, where simulations of temporal and spatial changes in LU/LC can provide important insights for preparing, developing, and evaluating regional and spatial plans [3,4]; the built environment, which comprises land use, urban design, infrastructure, and human activities within a physical area [5]; and natural and human-induced hazards, with respect to which there is a tendency, on a worldwide scale, to develop improved methodologies to deal with natural disasters as part of regional planning practices, especially where settlements (urban or rural) have already been established without consideration of the natural risks in the physical area [1].

Linking these spatial patterns to population trends, natural landscapes [6], hazards, and geomorphological features has been the focus of several studies. These investigations are usually carried out using remotely sensed data and GIS techniques that can detect, map, and evaluate changes over space and time [7–11]. This approach can be related to disaster risk reduction (DRR), which comprises both hazard mitigation and regional planning DRR should be designed in a way that is oriented to a population's aptitude to manage its built environment in a manner that is adjusted to cope with the natural and social environments [12]. The relationship between DRR and regional planning is well established. The built environment and the way it is designed can lead to disasters, especially in communities where planning policies and regulations are not usually well-enforced by local municipalities or councils [13,14].

This particularly proactive approach is referred to as "non-structural mitigation" of DRR. It is concerned with directing new built environment practices away from known and documented hazards through well-guided planning and policies, or relocating existing built environment developments toward safer areas while maintaining protective natural features, such as forests and green surfaces [15]. This approach is also in line with United Nations Sustainable Development Goal (SDG) 11, which aims at *"Making cities and human settlements inclusive, safe, resilient and sustainable"* [16], and with the Sendai Framework for Disaster Risk Reduction (2015–2030).

Built environment vulnerability and proneness to natural hazards have been the subject of several studies [14,17,18]. Changes in a built environment usually result in changes in land use [8,19] and may lead to deforestation. If not well planned, such changes may trigger natural hazards, e.g., landslides and destructive floods [19,20]. The interrelationship between landslides, built environments, population growth, and deforestation has been reported in several studies [14,21]. Holcombe et al. [14] concluded that unplanned built environments, especially in low-income communities, can lead to landslides, as urbanization and construction can have a destructive behavior toward unstable landmasses along slopes.

In Jordan, a country with a rich history of human occupation that dates back thousands of years [22], the population has increased rapidly over the past several decades, from about 230,000 in 1921 to 10,806,000 in 2020 [23], due to natural population growth and the influx of refugee [24]. This increase has decreased agricultural lands and increased unplanned built environments [8,11], adding pressure on natural resources [25]. Thus, the resulting built-environment practices and population increases in parts of Jordan are random [8,26] and haphazard, following a concentrated urban pattern rather than a pattern that is well-spread over the geographic areas [27].

One of the most important geohazards in Jordan is landslides, which are considered to be a third-priority natural disaster based on the Jordan National Natural Disaster Risk Reduction (JNDRR) Strategy (2019–2022). Several studies have concluded that landslides in Jordan are the result of the geological characteristics, tectonic settings, and morphological characteristics of the area; nonetheless, they have emphasized that anthropogenic activities have accelerated their occurrences [28–34].

This study presents new data regarding regional planning in Jordan, as reflected by changes in the built environment and its relationship with landslide events in the area between Amman and Jarash, alongside the Amman-Jarash highway, for the period 1994–2020, using satellite images, GIS, and statistical techniques. We also evaluate the relationship between geomorphological features and changes over time and space. In addition, this study provides a comprehensive geodatabase for the current built environment and social services, relative to landslide locations, to aid in the future planning in the area and to minimize the risk of future catastrophic losses in lives and property.

2. Study Area

The study area is located between the Amman and Jarash governorates (Figure 1), specifically from Jarash in the north to Mubis in the south and from Al Aluk in the east to Al Jazzaza in the west. The study area extends over parts of the Zarqa, Balqa, and Jarash governorates. The study area covers an area of approximately 270 km^2. The area comprises several landmarks, including King Talal Dam, and Wasfi Tal Forest, as well as several settlements with varying population sizes.

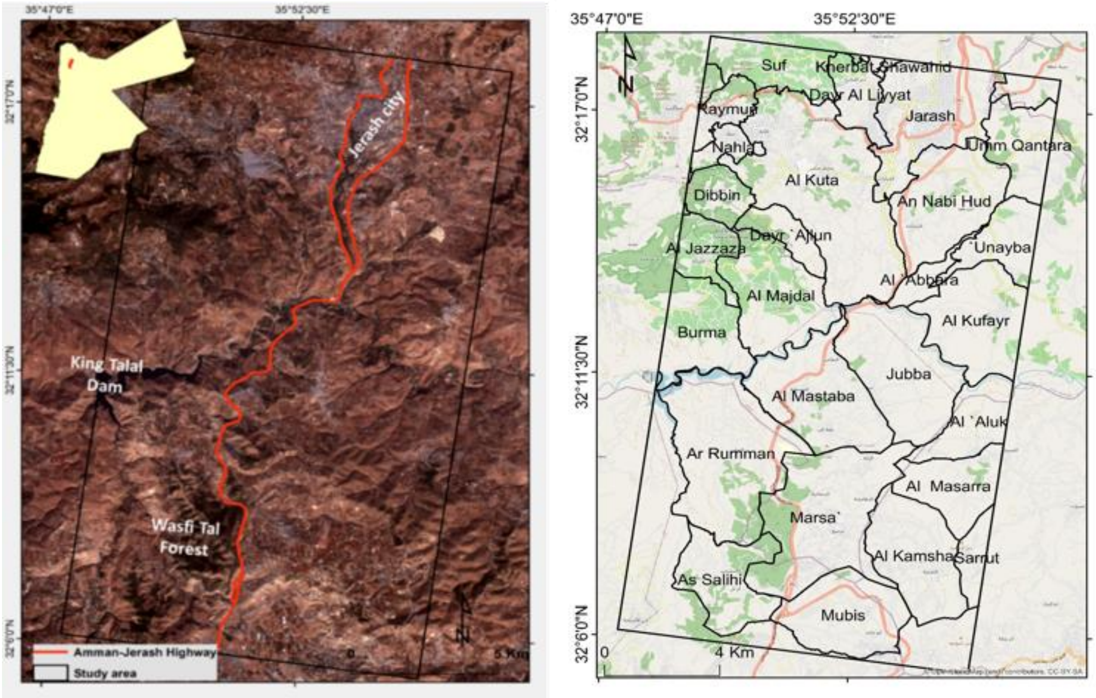

Figure 1. Left: study area location overlay a Sentinel-2 image. Image source: USGS earth explorer. Right: study area location overlay OpenStreetMap Standard Map (from https://www.openstreetmap.org/ (accessed on 15 July 2022)).

The built environment in the study area comprises built-up land, social services, green areas (forests and agricultural lands), and water bodies.

Based on data collected from the respective municipalities (Jarash and Bab Amman), the area comprises 24 settlements (Table 1). A major feature in the study area is the Amman–Jarash highway that passes through the old Amman–Syria highway (Figure 1).

Table 1. Populated settlements in the study area based on data from the respective municipaliteis and the Jordan Department of Statistics.

Admin Area	Population 2020	Admin Area	Population 2020
Jubba	5249	**Suf**	21,243
An Nabi Hud	2016	**'Unayba**	316
Al 'Abbara	227	**Al Kuta**	46,206
Al Kufayr	2788	**Raymun**	8804
Marsa'	5166	**Dibbin**	243
Ar Rumman	2250	**Jarash**	57,434
Mubis	9657	**Dayr Al Liyyat**	3253
As Salihi	1309	**Nahla**	4459
Al Mastaba	5529		
Al Majdal	491		
Sarrut	2114		
Al Kamsha	2407		
Al Jazzaza	1553		
Burma	6855		
Al 'Aluk	1365		
Al Masarra	1412		

The administrative areas represent both urban and rural settlements. The areas with more than 5000 people include Jarash City, AlKuta, Raymun, Jubba, Marsa', Mubis, Al Mastaba, and Burma, while the rest of the settlements are rural, with fewer than 5000 people.

3. Materials and Methods

The study methodology included collecting relevant literature and required datasets, as follows:

- Digital Elevation Model (DEM) SRTM v3 (30 m resolution) and satellite images (Landsat 5TM and Landsat 8OLI/TIRS) were downloaded from the USGS website (https://earthexplorer.usgs.gov/) accessed on 2 April 2021 and the Glovis website (https://glovis.usgs.gov/app) accessed on 2 April 2021.
- Administrative areas' geographical borders were obtained from the respective municipalities of Bab Amman and Jarash.
- Census data for 1994, 2004, 2015, and 2020 were downloaded from the website of the Department of Statistics in Amman, Jordan (http://dosweb.dos.gov.jo/) accessed on 26 March 2021.
- Administrative areas' (in km^2) data was obtained from the website of the Department of Statistics in Amman, Jordan (http://dosweb.dos.gov.jo/) accessed on 26 March 2021.
- Social services data were obtained from the Ministry of Education (schools), the Ministry of Health (health centers), and Civil Defense (civil defense centers) in the Jordan websites and via the use of Google Earth Pro Software.

The data was then preprocessed based on the intended analyses, tabulated, and saved in proper formats using Excel spreadsheets, shapefiles, etc. For the detailed methodologies used in this study, see Supplementary Materials File S1.

3.1. Built Environment Parameters

Together with GIS spatial analysis tools, such as choropleth maps, point density maps, heat maps, and directional distribution ellipses, which are useful in understanding the spatial and temporal variability in population size and growth rates, remote sensing (RS) data obtained through satellite remote sensing (SRS) are important in mapping different built-environment parameters [35–40].

Several indices have been developed to extract desired features and maps from RS data. Of these, the normalized difference vegetation index (NDVI) is the most widely used to extract vegetation cover [37,41,42]. In addition, built-up land can be observed and its changes can be monitored using image classification tools in ArcMap Software [8].

3.1.1. Population Size and Growth Rate: Spatial and Temporal Variations

For this component, a descriptive analytical approach was applied. The administrative boundaries data and the census data were obtained from the respective governmental directorates for the towns in the study area. The data were then tabulated and inserted into Microsoft Excel software for statistical analysis and to calculate the population growth rates. The data were then put into a GIS environment (ArcMap 10.8.1) to generate maps that showed the populations' temporal/spatial distribution, the growth rates' spatial distribution, the population density, the mean center point of population, and the directional distribution-standard deviation ellipses for 1994, 2004, 2015, and 2020.

3.1.2. Built-Up Land Changes

Following the study of Al Rawashdeh et al. [8], Landsat images were used to detect temporal and spatial changes in built-up areas and to calculate their areas and percentages over the studied time periods. Landsat data were inserted into ArcMap software and, using digital image processing tools, the built-up lands were mapped by supervised classification. The color combination of bands 4 (red), 3 (green), and 2 (blue) was used for this step. In this color combination, the built-up land appears in cyan color, while vegetation appears in red and green colors and water appears in black [41]. Because the focus is on delineating built-up lands, the on-screen digital image processing focused the training sample points on identifying areas with cyan color. Built-up (urban) areas typically comprised industrial and commercial buildings, residential development areas, and transportation facilities [41].

3.1.3. Green Surface Changes (Using NDVI)

NDVI [41] depends on the chlorophyll absorption of visible light and the reflectance of near infrared by the plant leaves and the cellular structures. Because satellite images are composed of bands that reflect different parameters of an image collection, measuring the difference between near infrared (NIR) and red bands in a satellite image provides an indication of the presence of chlorophyll and, thus, vegetation [39,42]. In ArcMap, the images were pre-processed (Supplementary Materials File S1) and Formula (1) was applied, using the spatial analysis tool "raster calculator".

$$\mathrm{NDVI} = \mathrm{NIR} - \mathrm{RED}/\mathrm{NIR} + \mathrm{RED} \tag{1}$$

The resultant index has values ranging from −1 to 1. Values <1 indicate water or snow; values <0.1 and >0 reflect empty areas, rocks, and sand. Values of about 0.1–0.3 indicate meadows and shrubs, while high values, >0.3, indicate vegetation [42].

For 1994 and 2004, Landsat 5 images were used, while the 2015 and 2020 NDVI calculations were based on Landsat8 imagery. The raster NDVI maps were then reclassified and the areas for the index values were calculated as pixel areas and then transformed into percentages. The NDVI maps and the calculated areas were measured for the subsequent time periods, 1994 to 2004, 2004 to 2015, and 2015 to 2020, to estimate the temporal and spatial variability in the green surfaces in the study area. Change detection in NDVI was calculated using the "Combine Tool" from the spatial analyst in ArcMap 10.8.1 software (version number 10.8.1.14362, Esri Inc., Redlands, CA, USA).

3.1.4. Social Services Mapping and Spatial Analysis for 2020

For the facilities and institutions mapping, online resources and Google Earth Software were used. The schools' data were downloaded from the Jordan Ministry of Education website [43] and mapped on Google Earth Pro 2020 software (version number 7.3.4.8642, Google Inc., Mountain View, CA, SA). The health centers' data were downloaded from the Jordan Ministry of Health website [44] and mapped on Google Earth Pro 2020 software. For the civil defense centers, data were digitized using Google Earth Pro Software. The data were then input into ArcMap 10.8.1 and transformed into shapefiles as part of a geodatabase for 2020. The data from this step were used as an input for the final map to show the present-day locations of the important social services in the study area, relative to the green surfaces, the built-up land, the population patterns, and the recorded landslides.

3.2. Landslide Spatial and Temporal Variability

To estimate landslide variability during the period from 1994 to 2020, the landslide event locations documented in the literature from 1994 to 2018 [28–31,33,34] were collected and the raw data were entered into ArcMap and transformed to shapefiles. Landslide maps were generated for 1994, 2004, and 2015. Then, the landslide events recorded in the media for 2019, 2020, and 2021 were added to the map to generate the final landslide map for 2020. A field trip was conducted to validate the 2020 landslide map, visiting the landslide locations and documenting them on the ground, using GPS readings and photographs. Finally, new landslide events were added to the map, which were located using Google Earth software and the fieldwork investigations.

3.3. Topographical Investigation

Topography plays a significant role in determining the distribution and change in land cover and population [11]. Thus, this study used DEM data and GIS techniques in order to calculate the elevation and slope in the study area. Based on the DEM data, the slope was calculated using the slope tool from the spatial analyst tools in ArcMap software.

Then, the raster data were converted to feature class (polygons) to calculate their areas and to estimate the spatial distribution of the elevation and slope. The "Union Tool" from the Arc Toolbox was then used to combine the different layers from previous analyses of the elevation (based on elevation scales used by Zreqat [11]), to investigate the effect of topography on the built-environment changes and the landslide events.

4. Results

4.1. Population Size and Growth Rates and Distribution Patterns during the Period 1994–2020

In order to better understand the population sizes, the descriptive statistics (Table 2) were calculated. The results for the study area as a whole showed that a high positive skewness (>2) was observed, which may affect any further investigations of population densities and distributions in which high values could mask smaller variations. To reduce this skewness, the study area was subdivided into two parts (northern and southern). The northern parts comprised the highest population sizes. The calculated descriptive statistics for the northern and southern parts showed lower enhanced skewness values of ~1 [45]. The population spatial and temporal analyses were conducted based on this subdivision in order to obtain better localized patterns.

Table 2. Descriptive statistics of the complete study area (northern parts and southern parts), showing better statistical parameters obtained after the study area's segmentation. POP: Population.

Study Area				
	POP_1994	POP_2004	POP_2015	POP_2020
Mean	3687.04	5194.04	7599.63	8014.42
Median	1149.5	1609	2294.5	2597.5
Skewness	2.3	2.37	2.59	2.82
Minimum	43	39	201	227
Maximum	21,278	31,652	50,745	57,434
Northern Parts				
	POP_1994	POP_2004	POP_2015	POP_2020
Mean	8500.88	12,124	17,223.13	17,744.75
Median	3699.5	4713.5	5859.5	6631.5
Skewness	0.59	0.65	0.93	1.19
Minimum	43	39	215	243
Maximum	21,278	31,652	50,745	57,434
Southern Parts				
	POP_1994	POP_2004	POP_2015	POP_2020
Mean	13,558.59	1812.41	2855.65	3226.29
Median	925	1239	1988	2250
Skewness	1.08	0.7	115	1.15
Minimum	341	326	201	227
Maximum	3725	4467	8531	9657

Population Growth Rates and Distribution Patterns

Table 3 lists the population growth rates for the settlements during the periods of 1994 to 2004, 2004 to 2015, and 2015 to 2020. The results showed that the population growth rates were not similar across the study area, probably due to unplanned practices observed in areas around Jordan [26,27], where some settlements had relatively high growth rates, while other settlements showed negative rates, probably reflecting the internal immigration effects that were common in Jordan, where people relocated to settlements with better economic potential [46]. The data showed that the main period with the highest population growth rate in the study area was from 2004 to 2015.

Table 3. Calculated population growth rates for the period from 1994 to 2020 in the study area. Note that population growth from 2015 to 2020 is based on a five-year period.

Southern Parts				Northern Parts			
Settlement	**Pop gr_94_04**	**Pop gr_04_15**	**Pop gr_15_20**	**Settlement**	**Pop gr_94_04**	**Pop gr_04_15**	**Pop gr_15_20**
Jubba	3.04	3.45	2.48	Suf	2.02	1.09	−4.69
An Nabi Hud	4.08	6.39	2.48	Unayba	0.37	12.24	2.49
Al Abbara	−0.45	−4.84	2.43	Al Kuta	5.04	4.31	0.49
Al Kufayr	3.22	3.33	2.48	Raymun	2.72	2.14	2.48
Marsa	3.11	3.79	2.47	Dibbin	−0.98	17.07	2.45
Ar Rumman	8.37	3.13	2.48	Jarash	3.97	4.72	2.48
Mubis	5.12	11.53	2.48	Dayr Al Liyyat	2.77	1.69	2.48
As Salihi	−1.67	3.9	2.49	Nahla	1.85	2.25	2.47
Al Mastaba	3.87	3.43	2.48	Average	2.22	5.69	1.33
Al Majdal	0.62	−3.5	2.47				
Sarrut	2.46	5.07	1.55				
Al Kamsha	5.05	5.4	2.48				
Al Jazzaza	1.44	1.52	2.48				
Burma	1.82	3.04	2.48				
Al Aluk	4.15	6.49	2.48				
Al Masarra	−1.31	8.69	2.49				
Average	2.68	3.8	2.42				

4.2. Built Environment and Landslide Changes (1994–2004)

Point density (heat) maps were generated for 1994 and 2004 (Figure 2). A general increase in the population size was noted, where the population increased from 1200 to 1400 and from 6800 to 10,000 people, respectively, in the southern and northern parts of the study area. The increase in population was higher in the northern parts, especially in the Jarash, Suf and Alkuta settlements, while the increase in the southern parts was mainly concentrated in Al-Mastaba, Burma, Jubba, and Mubis.

In terms of built-up land for 2004, the results (Figure 2b) indicated that built-up land covered 10.3% of the total area, a change of about 145% (Table 4) when compared to 1994 (4.2%). The increase was noted in all parts of the study area; however, it was particularly concentrated in Jarash, AlKuta in the north and central parts of the study area, around Jubba and AlMastaba, and to the south toward Amman. The built-up land and the population densities and directional distributions showed moderate similarity, probably indicating that population growth in the area was not directly linked to increases in built-up lands., such as developments in built-up lands and the resultant deforestation.

Table 4. Changes in built environment and landslide events during the period from 1994 to 2004.

Component	**Percent of Total Study Area (%)**		
	1994	**2004**	**Change (%)**
Built-up land	4.2	10.3	59.22
Green surfaces (NDVI)	16.6	16.4	−1.22
		Incidents	
Landslides	4	11	175

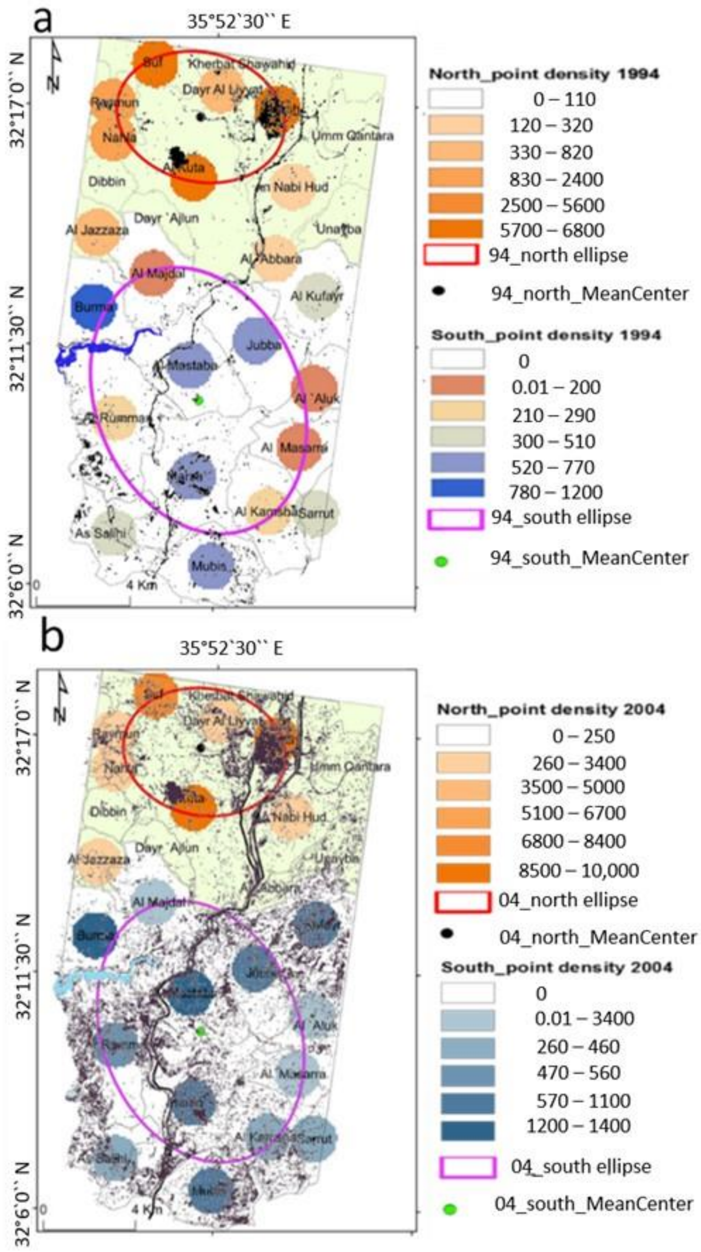

Figure 2. Heat maps (point density) showing the population concentration in the study area with the population directional distribution ellipses and the mean center points for 1994 (**a**) and 2004 (**b**). Superimposed is the built-up land map (black color).

In terms of vegetation changes, the NDVI analysis (Supplementary Materials File S2) for 1994 indicated that the green surfaces (>0.3 NDVI values) represented 16.6% of the total area (Figure S1). The values <0 that represented water that primarily reflecting the King Tala Dam. The green surfaces were primarily concentrated in Wasfi Tal Forest and in Debbin along the western and southern highlands, with some cover over the eastern parts of the study area and around the Dam and the Zarqa River. For 2004, the green surfaces covered similar areas (16.4%) (Figure S2), compared with 1994 where there was a slight decrease of −0.2% (change of −1.22%) (Table 4). The losses were primarily observed in the northern areas near Al Kuta, Jarash, and Raymun, in the central parts near AL Mastaba, and in the southern parts near As Salihi. The reduction in NDVI can be attributed to several reasons

For the landslide events, the results indicated an increase during this period. In 1994, only four landslide events were recorded in the literature. They were located in close proximity to Al Mastaba, Jubba, and Al Abbara, at elevations of 200 m asl to 500 m asl.

For 2004, the literature indicated that the landslide events increased to 11 incidents spread over a wider geographical area. The concentration of landslides was primarily within Al Mastaba and Al Abbara at the sides of the main highway. One landslide event was recorded in 2004, near Mubis in the south at an elevation of 500 m asl to 1000 m asl, while the rest of the landslides were at 200 m asl to 500 m asl. Landslide events during this time period increased by 175% (Table 4).

The built-up land distribution in 1994 was concentrated at elevations of 500 m asl to 1000 m asl (66.3%) and 200 m asl to 500 m asl (30.89%) (Table 5). Lowlands at <200 m asl comprised 1.08% of the total built-up lands, while the highlands, >1000 m asl, comprised the lowest percentage at 0.32%. These variations were also observed for the NDVI topographical distribution, where the highest NDVI percentage (>0.3 index) was concentrated at elevations of 200 m asl to 500 m asl and 500 m asl to1000 m asl with percentages of 40.95% and 35.23%, respectively. The lowest NDVI percentage was at <200 m asl, while 21.08% was detected at >1000 m asl. The lower percentages at <200 m asl might be the result of reduced precipitation rates, compared with higher elevations; the higher percentage at >1000 m asl might reflect forests at high altitudes. The concentration at 200 m asl to 1000 m asl, which was similar to built-up land concentrations, might reflect the role of agricultural activities in the study area [47].

Table 5. The influence of altitude on built-environment changes and landslide development during the period from 1994 to 2004. Built-up land and NDVI values are percentages of total index.

	Altitude (m asl)			
Built-up Land	**<200**	**200–500**	**500–1000**	**>1000**
1994	1.08	23.70	66.30	0.32
2004	1.61	30.89	74.90	1.20
Change %	49.07	30.34	12.97	275.00
NDVI				
1994	1.35	40.95	35.23	21.08
2004	17.10	30.73	24.00	25.34
Change %	1166.67	−24.96	−31.88	20.21
landslides				
1994	0.00	4.00	0.00	0.00
2004	0.00	8.00	3.00	0.00
Change %	0.00	100.00	300.00	0.00

However, in 2004 the built-environment spatial and topographical distribution varied. The built-up lands at altitudes <200 m asl increased by 49.07%; those at 200–500 m asl increased by 30.34%; those at 500 m asl to 1000 m asl, increased by 12.97%, and those at >1000 m asl increased by 275% (Table 5). The NDVI changes varied between positive and negative values, where NDVI at <200 m asl and at >1000 m asl increased by 1166.67% and 20.21%, respectively. The increase at elevations <200 m asl could be attributed to the lower Zarqa River development project (King Talal Dam) that started in 1997 ([11]), while the increase at >1000 m asl could be attributed to an increase in highland forests. On the other hand, NDVI decreased at altitudes of 200 m asl to 500 m asl and 500 m asl to 1000 m asl, by −24.96% and −31.88%, respectively. This decrease was associated with an increase in built-up land, probably reflecting the increase in population density and the associated urbanization and infrastructure construction, among other factors.

4.3. Built Environment and Landslides Changes (2004–2015)

Following the changes from 1994 to 2004, the next 11 years (2004 to 2015) showed the most distinctive changes in population trends in the study area. A substantial increase in the population size was recorded (Figure 3), with the highest average population growth rates of 3.8% and 5.69% for the southern and northern areas, respectively. The population sizes in the study area in 2015 increased from 1400 to 2700 and from 10,000 to 16,000 in the southern and northern parts of the study area, respectively. The population was mainly concentrated in the northern Jarash, Suf, and Alkuta settlements, while the increase in the southern parts was mainly concentrated in Al-Mastaba, Burma, and Mubis.

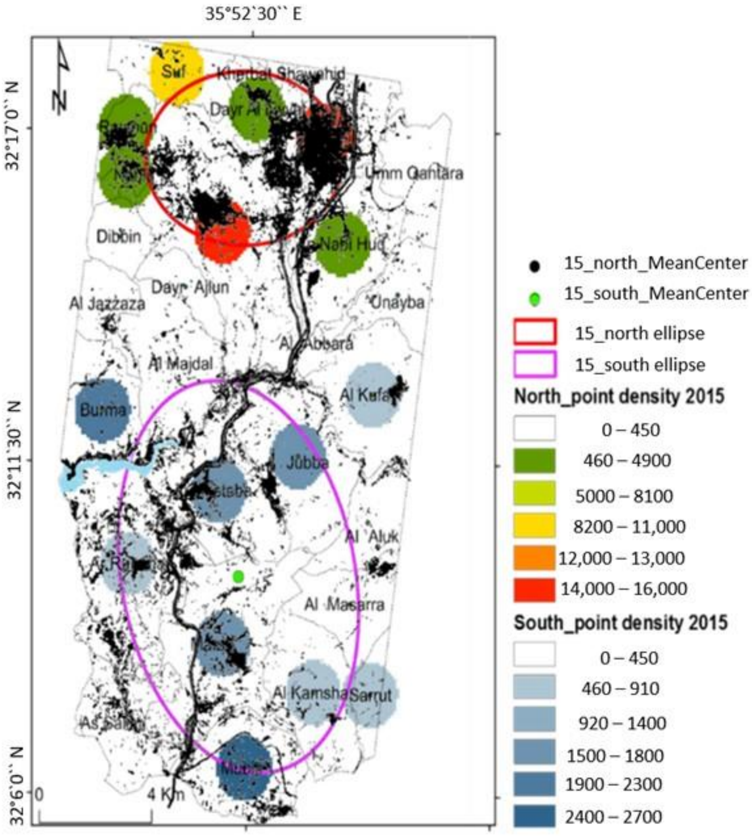

Figure 3. Heat maps (point density) showing the population concentration in the study area with the population directional distribution ellipses and mean center points for 2015. Superimposed is the built-up land map (black color). For the admin area borders and names refer to Figure 2b.

In terms of built-up land in 2015, the results showed that built-up land represented 14.34% of the total study area (Figure 3). The built-up land development was concentrated in Jarash, Alkuta, Raymun, and Debbin in the northern parts of the study area and to the southeast of Jarash in Nabi Hud, while it was concentrated in Al Mastaba, Jubba, Marsa', Ar Rumman, and Mubis in the southern parts, with increased built-up lands toward Amman and around King Talal Dam. In contrast with the observations for the period from 1994 to 2004, the built-up land and population densities showed good agreement where the built-up land primary concentrations were located within the population directional distribution ellipses, suggesting that population growth for this period was directly linked to increases in built-up lands.

The NDVI analysis (Supplementary Materials File S2) for 2015 indicated that the green surfaces (>0.3 NDVI values) represented 12.8% of the total area (Figure S4). The green surfaces were primarily concentrated in Wasfi Tal Forest and Debbin, along the eastern and southern highlands, with some cover over the eastern parts of the study area and around the Zarqa River. A decrease of 3.6% of the total green surface area was noted in the central and northern parts of the study area (Figure 4). This reduction accounted for a change of −21.95%. The results (Figure 4) showed that the losses in NDVI were primarily observed in the northern areas near Al Kuta, Jarash, An Nabi Hud, in the central parts near AL Mastaba, Jubba, Al Mastaba, and Marsa', and in the southern parts near As Salihi.

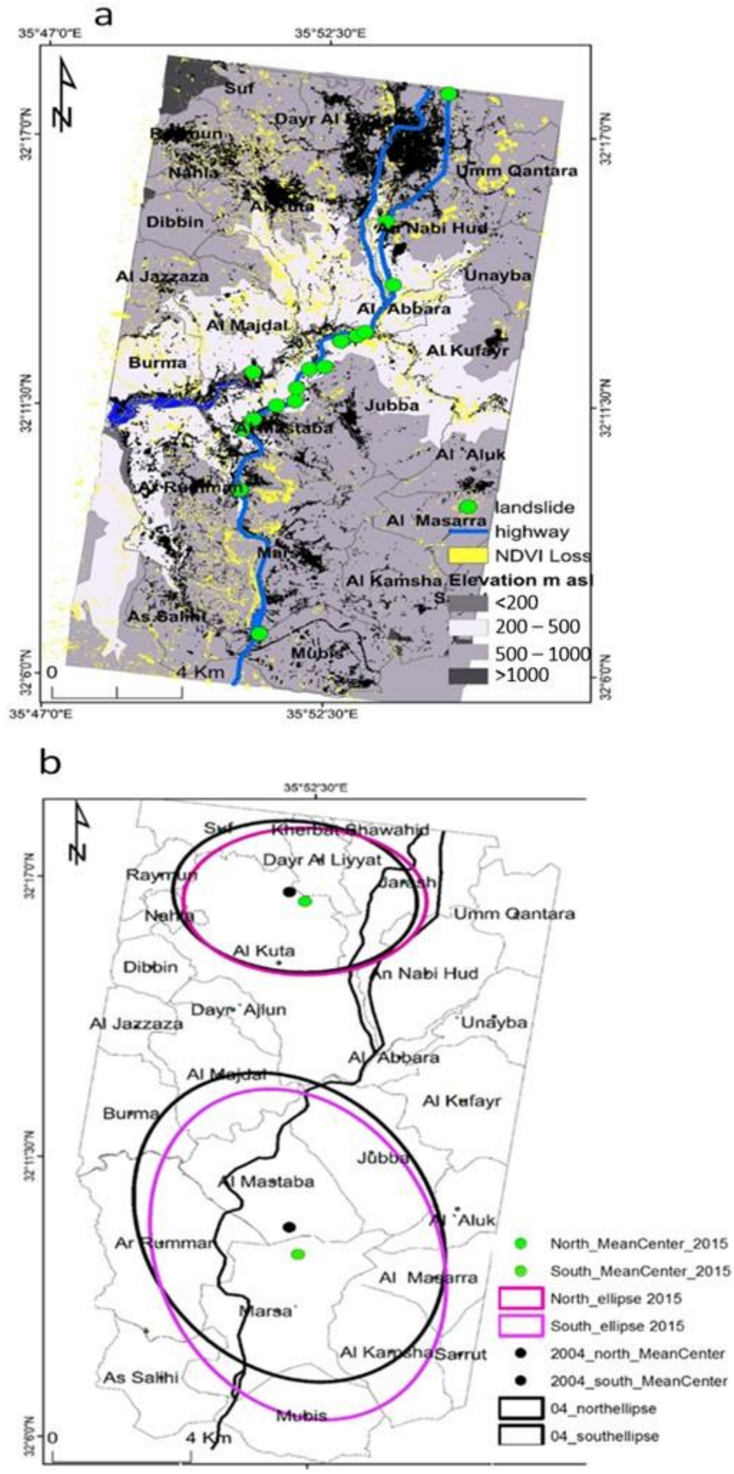

Figure 4. (**a**) Synthesis map showing the built-environment components, black: built-up land in 2015, yellow: NDVI loss. For the admin area borders and names refer to b; (**b**) illustration of the changes in population directional distribution and mean center points during the 11 years from 2004 to 2015.

Regarding landslide events, 16 locations were recorded in the literature for 2015 (Figure S5). The events were located close to Al Mastaba, Jubba, and Al Abbara. The concentration was primarily within Al Mastaba and Al Abbara at the sides of the main highway. One new event was recorded in the northern parts near Jarash. The landslides were found at altitudes of 200 m asl to –500 m asl and 500 m asl to 1000 m asl. Changes were observed at 200 m asl to 500 m asl. Additionally, one new event was recorded at <200 m asl. Landslide events during this time period increased by 45.45% (Table 6).

Table 6. Changes in built environment and landslide events during the period from 2004 to 2015.

Component	Percent of Total Study Area (%)		
	2004	**2015**	**Change (%)**
Built-up land	10.3	14.34	39.22
Green surfaces (NDVI)	16.4	12.8	−21.95
		Incidents	
Landslides	11	16	45.45

The built-up land distribution in 2015 in the study area was particularly concentrated at elevations of 500 m asl to 1000 m asl (54%) and 200 m als to 500 m asl (43.3%) (Table 7). Lowlands <200 m asl showed increased built-up area compared to 2004 and accounted for 5.4% of the built-up lands (total change of 235.4%), while the highlands >1000 m asl did not show significant changes (total change of 8.33%).

Table 7. The influence of elevation on built-environment changes and landslides development during the period from 2004 to 2015.

	Elevation (m asl)			
Built-Up Land	**<200**	**200–500**	**500–1000**	**>1000**
2004	1.61	30.89	74.9	1.2
2015	5.4	43.3	54	1.3
Change %	235.40	40.17	−27.90	8.33
NDVI				
2004	17.1	30.73	24	25.34
2015	25.5	28.6	21.8	24.7
Change %	49.12281	−6.93134	−9.16667	−2.52565
landslides				
2004	0	8	3	0
2015	1	13	3	0
Change %	100	62.5	0	0

4.4. Built Environment and Landslides Changes (2015–2020)

The period from 2015 to 2020 generally showed a slight change in population trends in the study area (Figure 5), with an average population growth rate of 2.42% and 1.33% for the southern and northern areas, respectively. The population sizes in the study area in 2020 (Figure 5) increased from 2700 to 3100 and from 16,000 to 18,000, respectively, in the southern and northern parts of the study area. The population was mainly concentrated in the northern Jarash and Alkuta settlements, while the increase in the southern parts was mainly concentrated in Al-Mastaba, Burma, and Mubis. In addition, based on the directional distribution and the mean center points of the population compared with those of 2015, no change in the southern parts was observed, while in the northern parts the concentration increased toward Jarash and AlKuta, moving the directional distribution in an anticlockwise movement to the southeast around the city of Jarash and the main highway (Figure 5).

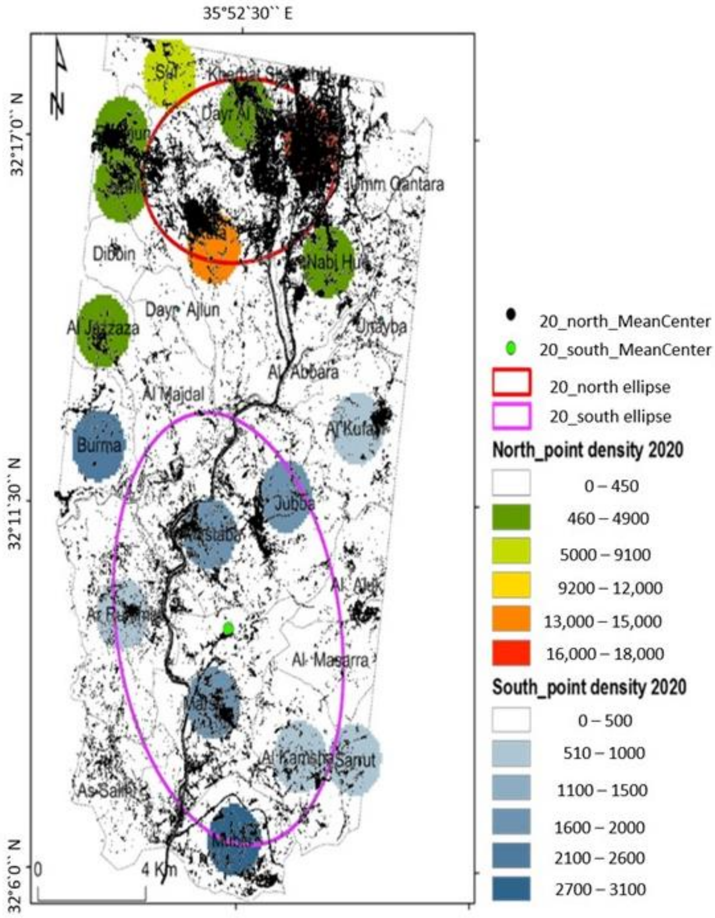

Figure 5. Heat map (point density) showing the population concentration in the study area with the population directional distribution ellipses and mean center points for 2020. Superimposed is the built-up land map (black color). For the admin area borders and names refer to Figure 4b.

For 2020, the results showed that built-up lands represented 18% of the total study area. The built-up lands (Figure 5) were concentrated in Jarash, Alkuta, and Raymun in the northern parts of the study area and to the southeast of Jarash in Nabi Hud, while they were concentrated in Al Mastaba, Jubba, Marsa', Ar Rumman, and Mubis in the southern parts, with increased built-up lands toward Amman and around King Talal Dam. The built-up land generally increased in most of the study area.

As was the case from 2004 to 2015, the built-up lands and the population densities from 2015 to 2020 showed good agreement where the built-up land concentrations were located within the population directional distribution ellipses, suggesting that population growth during this period was directly linked to increases in built-up lands.

The NDVI analysis for 2020 (Supplementary Materials File S2) (Figure S6) showed that the green surfaces (>0.3 NDVI values) represented 12% of the total area. The green surfaces were primarily concentrated in Wasfi Tal Forest and Debbin, along the eastern and southern highlands, with some cover over the eastern parts of the study area and around the dam and the Zarqa River. The decrease of 0.8% of the total green surface area represented a change of −6.2%. The results (Figure 6) showed that the losses were primarily in the northern areas near Al Kuta, in the north-western highlands, in the central parts near AL Mastaba, Jubba, and in the southern parts near Marsa'. The reduction in NDVI indicated reduced green surfaces in the resultant locations, which can be attributed to several factors, such as developments of built-up lands and the resulting deforestation.

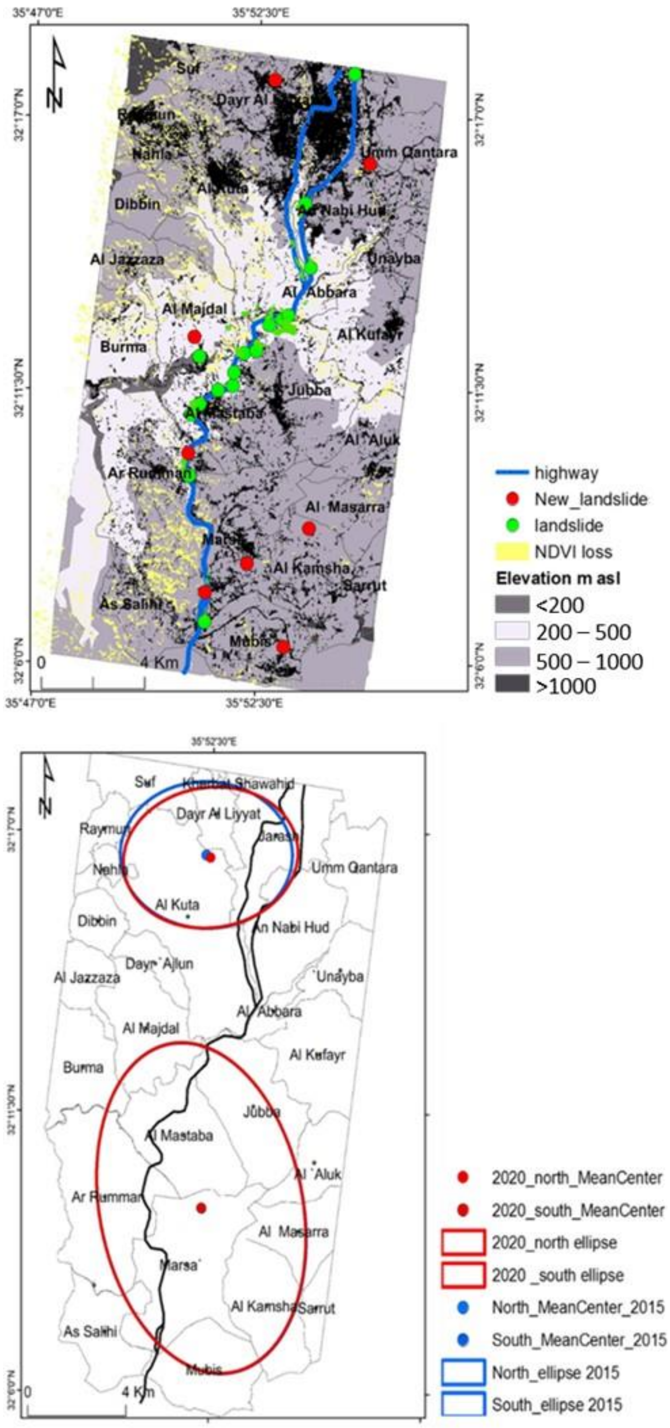

Figure 6. Top: synthesis map showing the built environment components. Black: built-up land 2020. For the admin area borders and names refer to bottom. Bottom: illustration of the change in population directional distribution and mean center points in the study area during the period from 2015 to 2020.

During the period from 2015 to 2020, six new landslide locations were recorded in the literature (Figure S7). However, it is worth mentioning that the previous studies focused on investigating landslide events at the sides of the main highway and did not provide comprehensive investigations of the complete study area.

Using GE Software and fieldwork, new landslide events were recorded away from the main highway (Figures S7 and S8). The landslide events were primarily concentrated at altitudes of 200 m asl to 500 m asl and 500 m asl to 1000 m asl, while few events were recorded at lower altitudes, <200 m asl, following recent built-up land increases in the lower altitudes. Nonetheless, the main location where landslide events were recorded was the central area of the study, close to Al Mastaba, Jubba, and Al Abbara. Another area of interest was the southern part, where new landslide events were recorded in this study and where populated areas were present. Because the landslide events recorded in this study may not be representative of the period from 2015 to 2020 and the fact that they may have been present for longer periods, only three landslides located close to the main highway and the one at <200 m asl were considered, with the landslide locations from the literature, in the change calculations.

The built-up land distribution in the study area in 2020 was particularly concentrated at elevations of 500 m asl to 1000 m asl (64%) and 200 m asl to 500 m asl (25.1%) (Table 8). Lowlands, <200 m asl, showed increased built-up areas compared with 2015 and accounted for 13% (a total change of 140.7%), while the highlands, >1000 m asl, showed negative changes (a total change of −46%).

Table 8. The effect of elevation on built-environment changes and landslide development during the period from 2004 to 2015.

	Elevation (m asl)			
Built-up Land	**<200**	**200–500**	**500–1000**	**>1000**
2015	5.4	43.3	54	1.3
2020	13	25.14	64	0.7
Change %	140.74	−41.94	18.52	−46.15
NDVI				
2015	25.5	28.6	21.8	24.7
2020	19.6	30.4	25.13	28.85
Change %	−23.1373	6.293706	15.27523	16.80162
landslides				
2015	1	13	3	0
2020	1	21	3	
Change %	100	61.54	0	0

5. Discussion

During the studied time period from 1994–2020, the population densities varied, resulting in changed urban and rural settlements in the study area. The area's population size increased from 88,489 people in 1994 to 192,346 people in 2020, a total change of 117.4%. Similar to other areas in Jordan [11,27,48,49], the population distribution in the study area has not been well-planned; it is unequal in terms of the spatial distribution, with more than 50% of the total population concentrated in about 25% of the total physical area (Figure 7). It has been reported for Amman, Jordan [49], and Asfahan, Iran [50], that in main cities, rapid urbanization can be influenced by the presence of either main roads or agricultural lands. Similarly, this study showed that the population distribution of the study area is generally expanding near the main highway, which indicates the significance of the main highway in attracting people to the area. In addition, the population seems to be moving toward the main cities in the north and south, closer to Jarash and Amman, respectively. Considering the long-term direction of the population distribution, clockwise and anticlockwise in the southern and northern parts of the study area, respectively, the population distribution ellipse is expected to lie along the same north–south axis and to concentrate near the main highway in the future (Figure 7), if these practices are not managed.

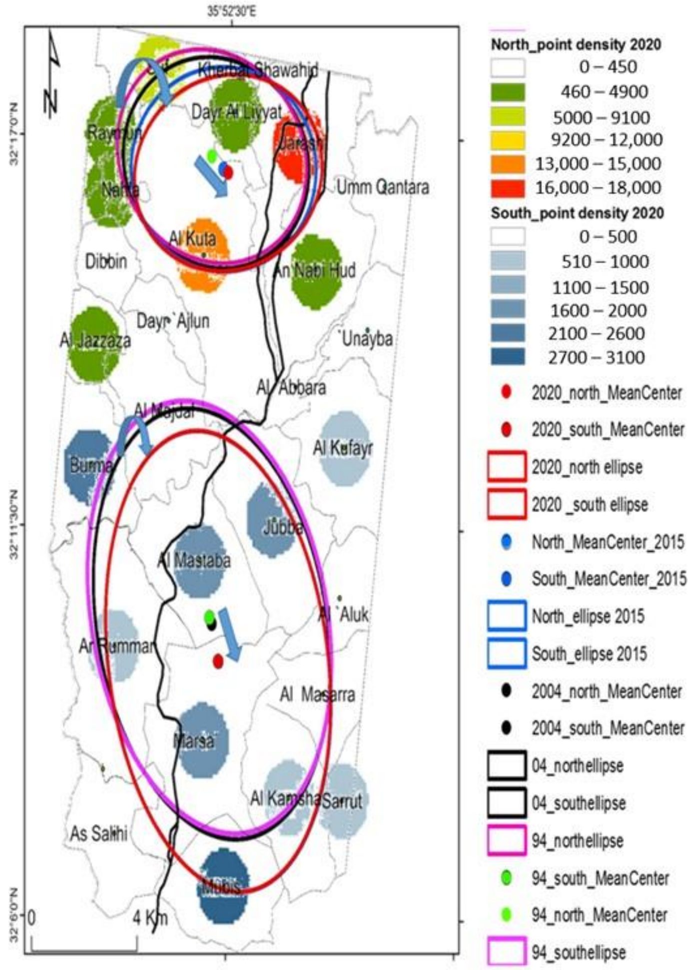

Figure 7. Map illustrating the comprehensive change in population dynamics for the period from 1994 to 2020.

Land use planning is essential in building cities that are resilient against present and potential natural risks [51]. It has been reported in different regions around the world that urbanization can be a major driver of natural hazards. In Sierra Leone, Cui et al. [20] reported that unplanned urbanization in environmentally vulnerable areas led to a destructive landsliding incident that resulted in more than 500 deaths. Similarly, temporal and spatial associations have been linked to population dynamics, built-up land increases, NDVI decreases, and the development of landslides in the study area. The results for the period from 1994 to 2004 indicate that the most significant changes in land cover (built-up land and green surfaces) in the study area took place at altitudes of 200 m asl to 1000 m asl. There were also increases in landslides at altitudes of 200 m asl to 500 m asl and 500 m asl to 1000 m asl, by 100% and 300%, respectively (Figure S3), suggesting that the built environment was probably a major factor in landslide occurrences during this period. Built-up lands substantially increased in Jarash, Suf, Al Kuta, Al Mastaba, Burma, Jubba, and Mubis. This increase was associated with a decrease in NDVI index values, emphasizing the relationship between the built environment and the natural environment and suggesting that the built environment played a significant role in the development of landslides in the area during this period. Unlike the situation in 2004, in 2015, a negative change occurred in built-up lands at altitudes 500 m to 1000 m, which probably reflected the tendency during this period toward agricultural activities at lower altitudes closer to irrigation water resources, such as the Zarqa River and King Talal Dam, which contributed to the increase in built-up lands at lower altitudes. These variations were also observed for NDVI topographical distribution, where the highest NDVI percentage for 2015 was concentrated at elevations of 200 m asl to 500 m asl and at <200 m asl, with percentages of 28.6% and 25.5%, respectively. The lowest NDVI percentage was at 500 m asl to 1000 m asl, while 24.7% was detected at >1000 m asl. The increase in NDVI percentages at <200 m asl supports the suggestion of the tendency toward agricultural activities in lower areas. This is also supported by a negative change in NDVI between 2004 and 2015 at altitudes of 200 m asl to >1000 m asl.

In 2020, a negative change was noted in built-up lands at altitudes 200 m asl to 500 m asl, probably reflecting the tendency during this period toward built-up land changes at lower and higher altitudes. These variations were also observed for the NDVI topographical distribution, where the highest NDVI percentage for 2020 was concentrated at elevations of 200 m asl to 500 m asl and >1000 m asl, with percentages of 30.4% and 28.85%, respectively. The lowest NDVI percentage was at <200 m asl, while 25.13% was detected at 500 m asl to 1000 m asl. The increase in NDVI percentages at altitudes higher than 200 m asl probably reflected the growing season effect, as the Landsat images that were used were downloaded between May and June. A negative change in NDVI was recorded for the altitudes higher than 200 m asl, with a total change of −23.13%. The landslide events were primarily concentrated at altitudes of 200 m asl to 500 m asl and 500 m asl to 1000 m asl, while few events were recorded at altitudes lower than 200 m asl, following a recent increase in built-up land in the lower altitudes, resulting in an NDVI increase of 56.25%.

Current State of the Study Area

Social services planning is considered to be one of the primary objectives of regional planning [52]. This study analyzed the spatial planning practices of health centers, government schools (social services), and civil defense centers (administrative services) in the study area.

Based on data acquired from the Jordan Ministry of Education, the study area comprised 110 government schools (Figure S9). The schools included elementary level, secondary level, and high schools. The average nearest neighbor tool in ArcMap was used to investigate the schools' distribution patterns. The results indicated that the schools' nearest neighbor ratio was 0.512, with a z-score of −9.8 and a p value of <0.01. Considering the z-score, the schools distributio'n pattern was considered as clustered. This agrees with the unequal spatial distribution of the population, as discussed earlier. Most of the schools are located at 500 m asl to 1000 m asl, while few are located in the 200 m asl to 500 m asl altitude regions. It is noted that the density of schools (number of schools in one physical area) follows the population density, where more schools are spatially located in urban settlements with >5000 people (e.g., Jarash, Suf Al Mastaba), while fewer schools are found in rural settlements with <5000 people (e.g., Al Aluk, Al Kufayr). Most of the schools are located at slopes with values of 8% to 20%; a few schools are located at slope ranges of 21% to 55%, and others are located at slope ranges of 3% to 7%. This is significant, considering that the landslide events in the study area were found primarily at altitudes of 200 m asl to 500 m asl and to lesser extent at 500 m asl to 1000 m asl and at <200 m asl. In addition, the landslides were found at slopes >21%.

For the health services (Figure S10), the results indicated that the nearest neighbor ratio was 1.299 with a z-score of 3.02 and a p value of <0.01. Considering the z-score, the health services distribution pattern was considered as dispersed. This agreed with the unequal spatial distribution of the population densities and the distances between settlements in the study area. The health centers are located at 500 ma asl to 1000 m asl. It is noted that the density of health services follows the population density, where more services are spatially located in urban settlements with >5000 people (e.g., Jarash, Suf Al Mastaba), while less are found in rural settlements with <500 people (e.g., Al Aluk, Al Kufayr). Most of the health services are located at slopes with values of 8% to 20%; a few are located at slope ranges of 21% to 55% and others are located at slope ranges of 3% to 7%.

Based on the GE Software survey, the study area included four civil defense departments (Figure S11). The departments were located at elevations of 500 m asl to 1000 m asl and at slope ranges of 8% to 21%. The distribution shows that they were concentrated in the northern parts of the study area, close to vegetated zones and the main cities of Jarash and Suf. Their locations indicated that they were located far from recorded landslide events. Their distribution probably followed the main population densities that were higher in the northern parts.

A comprehensive map illustrating the temporal and spatial changes in the population directional distribution and mean center points, the current built-environment components, and the landslide events in the study area was created (Figure 8) in order to assess the current planning practices and to draw on the relationship between these practices and the natural hazard locations in assessing the role of regional planning in monitoring built-environment changes and reducing natural hazard risks to ensure safer and more sustainable cities and settlements. The results indicate that the built-up environment practices in the study area are not well-planned in terms of the consideration of natural risks (e.g., landslides) and their potential hazardous impacts. As observed by the changes in built-up lands based on altitude, changes took place during periods when national projects were in operation, indicating that the economic factor is significant in driving these changes. In addition, the results indicated that the reduction in NDVI is associated with increased built-up lands in different areas, suggesting that urbanization is causing deforestation in the study area. The results also proved that whenever the built-up land increased, landslide events occurred, at certain times associated with a reduction in NDVI. This study agrees with previous studies that reported significant built-up and land cover changes in Jarash [11], Burma [48], and Amman [41,49], where significant built-up land development was recorded, and with a study [33] that provided a detailed map of zones that are highly susceptible to landsliding along the Amman–Jarash Highway.

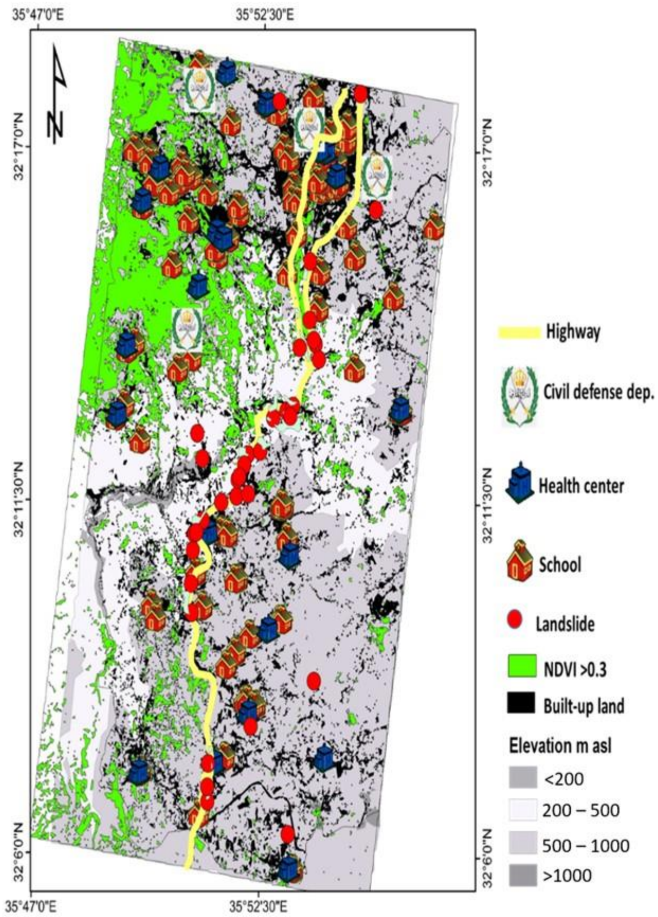

Figure 8. Comprehensive current state of the study area showing the built-environment components and the landslide locations for 2020.

6. Summary and Conclusions

The results of this study indicate the need for better regional (spatial) planning practices in the study area, in which the occurrence of natural hazards and the most susceptible altitudes and slopes would be considered in the planning of population distribution, future built-up land developments, services, and the development of green surfaces. The results provide support for decision-makers and scientific evidence that can be applied to future regional planning in the study area.

It is suggested that the built-up environment in the southern parts of the study area be planned and moved in an east–west direction rather than in a north–south direction, while considering the slope and altitude distribution in the study area and avoiding high slopes that are susceptible to landslides. It is suggested that in the northern parts of the study area, the built environments and the population distributions be planned away from landslide concentration areas and from the highway. In addition, it is suggested that the main highway should attract populations along its sides, as it offers good economic potential. Public awareness about settling close to such highway areas is also crucial in achieving more resilient and safer settlements and more effective regional planning strategies.

These observations indicate the significance of regional planning in monitoring and studying temporal and spatial changes in the built environment and linking these changes to natural hazards, a concept that is not well-practiced as part of regional planning in Jordan.

For example, based on data from the Jordan General Budget Department (GBD) [53], the following four projects have been approved for the Jarash governorate: (1) the construction and reconstruction of farm roads in Jarash, with a projected cost of JOD 3,000,000; (2) the construction and enhancement of the main and secondary village roads, with a projected cost of JOD 1,400,000; (3) the rehabilitation of the forested lands in Jarash, with a projected cost of JOD 150,000; and (4) the rehabilitation of 30% of the Debbin natural forest areas that are subject to fire hazards, with a projected cost of JOD 30,000. The planning processes for these projects should include consideration of the outcomes of this study, and include natural hazards as part of infrastructure planning and as a guide in identifying the areas with the most suitable and urgent needs for vegetation.

Supplementary Materials: Supporting information can be downloaded at: https://www.mdpi.com/article/10.3390/su14159241/s1, File S1. Detailed Methodology of the Study [11,28–42,54–58]. File S2. Detailed Maps of the Study: Figure S1. NDVI map of the study area for the year 1994. Figure S2. NDVI map of the study area for the year 2004. Figure S3. Landslide locations for the years 1994/2004 (for data sources see the main text), superimposed on DEM data. Figure S4. NDVI map of the study area for the year 2015. Figure S5. Landslide locations for the year 2015 (for data sources see the main text), superimposed on DEM data. Figure S6. NDVI map of the study area for the year 2020. Figure S7. Landslide locations for the year 2020 (for data sources see the main text), superimposed on DEM data. Figure S8. New Landslide (NL) 5 and 6 events recovered from the fieldtrip and Google Earth survey. Also showing the landscape change over a period of 10 years (2010–2020). Figure S9. Schools spatial distribution in the study area and population densities superimposed on the DEM. Figure S10. Left: Health Centers spatial distribution in the study area superimposed on the DEM. Right: Health Centers spatial distribution in the study area and landslide locations superimposed on the slope map. Figure S11. Left: Civil Defense departments spatial distribution in the study area superimposed on the DEM. Right: Civil Defense departments' spatial distribution in the study area and landslide locations superimposed on the slope map.

Author Contributions: Conceptualization, R.Q. and T.A.-A.; methodology, R.Q. and T.A.-A.; software, T.A.-A.; formal analysis, R.Q. and T.A.-A.; investigation, T.A.-A.; resources, R.Q.; data curation, T.A.-A.; writing—original draft preparation, T.A.-A.; writing—review and editing, R.Q.; visualization, R.Q. and T.A.-A.; supervision, R.Q. All authors have read and agreed to the published version of the manuscript.

Funding: This research received no external funding.

Institutional Review Board Statement: Not applicable.

Data Availability Statement: Not applicable.

Acknowledgments: The authors would like to thank Mahmoud Al-Habees and Marwan Al-Nsour for their valuable discussions and comments that significantly improved this study. The authors would also like to thank the editor and three anonymous reviewers for their positive feedback and comments that improved this manuscript. The authors would also like to acknowledge that the map data in Figure 1 (right) is copyrighted OpenStreetMap contributors and available from https://www.openstreetmap.org (accessed on 15 July 2022).

Conflicts of Interest: The authors declare no conflict of interest.

References

1. Gonzalez-Mathiesen, C.; March, A. *Developing Guidelines for Increasing the Resilience of Informal Settlements Exposed to Wildfire Risk Using a Risk-Based Planning Approach*; Santos, P.P., Chmutina, K., Meding, J., Von Raju, E., Eds.; Understanding Disaster Risk; Elsevier: Amsterdam, The Netherlands, 2021; pp. 159–178.
2. Eggenberger, M.; Partidário, M.R. Development of a framework to assist the integration of environmental, social and economic issues in spatial planning. *Impact Assess. Proj. Apprais.* **2000**, *18*, 201–207. [CrossRef]
3. Hietel, E.; Waldhardt, R.; Otte, A. Analyzing land-cover changes in relation to environmental variables in Hesse, Germany. *Landsc. Ecol.* **2004**, *19*, 473–489. [CrossRef]
4. Koomen, E.; Koekoek, A.; Dijk, E. Simulating Land-use Change in a Regional Planning Context. *Appl. Spat. Anal. Policy* **2011**, *4*, 223–247. [CrossRef]
5. Handy, S.L.; Boarnet, M.G.; Ewing, R.; Killingsworth, R.E. How the built environment affects physical activity: Views from urban planning. *Am. J. Prev. Med.* **2002**, *23*, 64–73. [CrossRef]
6. Brookes, C.J. A genetic algorithm for designing optimal patch configurations in GIS. *Int. J. Geogr. Inf. Sci.* **2001**, *15*, 539–559. [CrossRef]
7. Harris, P.M.; Ventura, S.J. The integration of geographic data with remotely sensed imagery to improve classification in an urban area. *Photogramm. Eng. Remote Sens.* **1995**, *61*, 993–998.
8. Al Rawashdeh, S.; Saleh, B. Satellite Monitoring of Urban Spatial Growth in the Amman Area, Jordan. *J. Urban Plan. Dev.* **2006**, *132*, 211–216. [CrossRef]
9. Al-Habees, M. Spatial Development Disparity in Jordan. *Jordan J. Soc. Sci.* **2011**, *4*, 180–202.
10. Btoush, N. Recent Trends of Population Growth and their Consequences in Jordan. *Jordan J. Soc. Sci.* **2012**, *5*, 11–124.
11. Zreqat, D. Land Cover Change in Jerash Governorate between (1952–2009) Using Geographic Information Systems (GIS) and Remote Sensing (RS). *Jordan J. Soc. Sci.* **2014**, *7*, 60–81.
12. Wamsler, C. Managing urban risk: Perceptions of housing and planning as a tool for reducing disaster risk. *Glob. Built Environ. Rev.* **2004**, *4*, 11–28.
13. Ofori, G. Construction Industry Development for Disaster Prevention and Response. In Proceedings of the i-Rec Conference on Improving Post-Disaster Reconstruction in Developing Countries, Montreal, QC, Canada, 23–25 May 2002; pp. 1–21.
14. Holcombe, E.A.; Beesley, M.E.W.; Vardanega, P.J.; Sorbie, R. Urbanisation and landslides: Hazard drivers and better practices. *Proc. Inst. Civ. Eng. Civ. Eng.* **2016**, *169*, 137–144. [CrossRef]
15. Godschalk, R. Urban Hazard Mitigation: Creating Resilient Cities. *Nat. Hazards Rev.* **2003**, *4*, 136–143. [CrossRef]
16. United Nations. *The 2030 Agenda and the Sustainable Development Goals: An Opportunity for Latin America and the Caribbean (LC/G. 2681-P/Rev. 3)*; United Nations: New York, NY, USA, 2018.
17. Wisner, B.; Blaikie, P.; Cannon, T.; Davis, I. *At Risk: Natural Hazards, People's Vulnerability and Disasters*, 2nd ed.; Routledge: London, UK, 2003; p. 496.
18. Smyth, C.G.; Royle, S.A. Urban landslide hazards: Incidence and causative factors in Niteroi, Rio de Janeiro state, Brazil. *Appl. Geogr.* **2000**, *20*, 95–118. [CrossRef]
19. Li, G.; Lei, Y.; Yao, H.; Wu, S.; Ge, J. The influence of land urbanization on landslides: An empirical estimation based on Chinese provincial panel data. *Sci. Total Environ.* **2017**, *595*, 681–690. [CrossRef] [PubMed]
20. Cui, Y.; Cheng, D.; Choi, C.E.; Jin, W.; Lei, Y.; Kargel, J.S. The cost of rapid and haphazard urbanization: Lessons learned from the Freetown landslide disaster. *Landslides* **2019**, *16*, 1167–1176. [CrossRef]
21. Chen, Y.; Xie, W.; Xu, X. Changes of Population, Built-up Land, and Cropland Exposure to Natural Hazards in China from 1995 to 2015. *Int. J. Disaster Risk Sci.* **2019**, *10*, 557–572. [CrossRef]
22. Patai, R. *Kingdom of Jordan, Princeton Legacy Library*; Princeton University Press: Princeton, NJ, USA, 2015.
23. Jordan Department of Statistics. 2020. Census report. Available online: www.dos.gov.jo (accessed on 26 March 2021).
24. Alhusban, A.; Alhusban, S.; Al-Betawi, Y. Assessing the impact of urban Syrian refugees on the urban fabric of Al Mafraq city architecturally and socially. *Int. J. Disaster Resil. Built Environ.* **2019**, *10*, 99–129. [CrossRef]
25. Salameh, E. Over-exploitation of groundwater resources and their environmental and socio-economic implications: The case of Jordan. *Water Int.* **2008**, *33*, 55–68. [CrossRef]
26. Alnsour, J.; Meaton, J. Factors affecting compliance with residential standards in the city of Old Salt, Jordan. *Habitat Int.* **2009**, *33*, 301–309. [CrossRef]

27. Quteishat, R.; Abu Sabha, K. Analyzing the Spatial Distribution of Jordanian Cities Using GIS. *Dirasat* **2014**, *41*, 529–554.
28. Malkawi, A.I.H.; Taqieddin, S.A. Geotechnical study of landslides resulting from a highway construction in Jordan. *Nat. Hazards* **1996**, *13*, 1–15. [CrossRef]
29. Mansour, Z.; Mustafa, H.; Abederahman, N. Geological and geotechnical studies of three main slides along Jerash–Amman highway. *Abhath AlYarmouk Pure Sci. Eng.* **1997**, *6*, 79–104.
30. Malkawi, A.; Saleh, B.; Al-Sheriadeh, M.; Hamza, M. Mapping of landslide hazard zones in Jordan using remote sensing and GIS. *J. Urban Plan Dev.* **2000**, *126*, 1–17. [CrossRef]
31. El-Naqa, A.; Abdelghafoor, M. Application of SINMAP terrain stability model along Amman–Jerash–Irbid highway, North Jordan. *Electron J. Geotech. Eng.* **2006**, *11*, 2–19.
32. Akawwi, E.; Al Assaf, A.; Barghouthi, A. Landslide, Rockfall Hazard Assessment and Risk Inventory Maps at South Jordan. *Int. J. Adv. Mech. Civ. Eng.* **2018**, *5*, 58–61.
33. Awawdeh, M.M.; ElMughrabi, M.A.; Atallah, M.Y. Landslide susceptibility mapping using GIS and weighted overlay method: A case study from North Jordan. *Environ. Earth Sci.* **2018**, *77*, 732. [CrossRef]
34. Masannat, Y.M. Landslide Hazards: Geotechnical Aspects and Management Policies. *Jordan J. Civ. Eng.* **2014**, *8*, 22. [CrossRef]
35. Lillesand, T.M.; Kiefer, R.W.; Chipman, J.W. *Remote Sensing and Image Interpretation*; John Wiley & Sons: Hoboken, NJ, USA, 2004.
36. Cyr, J.F.S. At risk: Natural hazards, people's vulnerability, and disasters. *J. Homel. Secur. Emerg. Manag.* **2005**, *2*, 1–7.
37. Jensen, J.R. *Remote Sensing of the Environment: An Earth Resource Perspective*, 2nd ed.; Prentice Hall: Upper Sadle River, NJ, USA, 2006.
38. Xu, H. A new index for delineating built-up land features in satellite imagery. *Int. J. Remote Sens.* **2008**, *29*, 4269–4276. [CrossRef]
39. Griffiths, P.; Hostert, P.; Gruebner, O.; van der Linden, S. Mapping megacity growth with multi-sensor data. *Remote Sens. Environ.* **2010**, *114*, 426–439. [CrossRef]
40. He, C.; Shi, P.; Xie, D.; Zhao, Y. Improving the normalized difference built-up index to map urban built-up areas using a semiautomatic segmentation approach. *Remote Sens. Lett.* **2010**, *1*, 213–221. [CrossRef]
41. Al-Bilbisi, H.; Tateishi, R. Using satellite remote sensing data to detect land use/cover changes and to monitor land degradation in central Jordan. *J. Jpn. Soc. Photogramm. Remote Sens.* **2003**, *42*, 4–18. [CrossRef]
42. Gandhi, G.M.; Parthiban, S.; Thummalu, N.; Christy, A. Ndvi: Vegetation Change Detection Using Remote Sensing and Gis—A Case Study of Vellore District. *Procedia Comput. Sci.* **2015**, *57*, 1199–1210. [CrossRef]
43. Jordan Ministry of Education. 2020. School in Jordan. Ministry of Education. Retrieved. 2020. Available online: http://www.e-daleel.gov.jo/. (accessed on 26 March 2021).
44. Jordan Ministry of Health. 2020. Health Centres. Retrieved. 2020. Available online: https://moh.gov.jo/AR/List/%D8%A7%D9%84%D9%85%D8%B1%D8%A7%D9%83%D8%B2_%D8%A7%D9%84%D8%B5%D8%AD%D9%8A%D8%A9. (accessed on 27 March 2021).
45. Cain, M.K.; Zhang, Z.; Yuan, K.-H. Univariate and multivariate skewness and kurtosis for measuring nonnormality: Prevalence, influence and estimation. *Behav. Res. Methods* **2017**, *49*, 1716–1735. [CrossRef] [PubMed]
46. Anbar, A.; Abu Sabha, K. Internal Migration in Jordan: Its Size, and Trends. *Jordan J. Soc. Sci.* **2009**, *2*, 211–255.
47. Alassaf, A.; Majdalwai, M.; Nawash, O. Factors affecting farmer's decision to continue farm activity in marginal areas of Jordan. *Afr. J. Agric. Res.* **2011**, *6*, 2755–2760.
48. Zreqat, D.; Alhusban, Y. Land Cover Changing Detection by GIS and Air Photographs: Bourma*, Sub-district of Jerash. *Jordan J. Soc. Sci.* **2012**, *5*, 1–14.
49. Al-Bilbisi, H. Spatial Monitoring of Urban Expansion Using Satellite Remote Sensing Images: A Case Study of Amman City, Jordan. *Sustainability* **2019**, *11*, 2260. [CrossRef]
50. Soffianian, A.; Ahmadiadoushan, M.; Yaghmael, L.; Falahatkar, S. Mapping and analyzing urban expansionusing remotely sensed imagery in Isfahan, Iran. *World Appl. Sci. J.* **2010**, *9*, 1370–1378.
51. Burby, R.J.; Deyle, R.E.; Godschalk, D.R.; Olshansky, R.B. Creating Hazard Resilient Communities through Land-Use Planning. *Nat. Hazards Rev.* **2000**, *1*, 99–106. [CrossRef]
52. Al-Habees, M. Spatial analysis of Health Centers in the Governorate of Amman, Jordan. *J. Med. J.* **2013**, *47*, 44–56. [CrossRef]
53. Jordan General Budget Department. 2022. List of Projects for the year 2022. Retrieved. 2022. Available online: http://gbd.gov.jo/Uploads/Files/gbd/law-min/2022/ar/4.pdf (accessed on 1 June 2022).
54. Bhatti, S.S.; Tripathi, N.K. Built-up area extraction using Landsat 8 OLI imagery. *GIScience Remote Sens.* **2014**, *51*, 445–467. [CrossRef]
55. Agung, I.N. Identical population estimates using the exponential and geometric growth functions. *Maj. Demogr. Indones* **1993**, *20*, 69–74.
56. Chander, G.; Markham, B.L.; Helder, D.L. Summary of current radiometric calibration coefficients for Landsat MSS, TM, ETM+, and EO-1 ALI sensors. *Remote Sens. Environ.* **2009**, *113*, 893–903. [CrossRef]
57. Firl, G.; Carter, L. *Calculating Vegetation Indices from Landsat 5 TM and Landsat 7 ETM+ Data*; Colorado State University: Fort Collins, CO, USA, 2011.
58. Vogelmann, J.E.; Howard, S.M.; Yang, L.; Larson, C.R.; Wylie, B.K.; Van Driel, J.N. Completion of the 1990s National Land Cover Data set for the conterminous United States from Landsat Thematic Mapper data and ancillary data sources. *Photogramm. Eng. Remote Sens.* **2001**, *67*, 650–662.